Evaluation of a North Atlantic 1/12° model simulation

Raphael Dussin and Anne Marie Treguier *

LPO Report LPO-2008-07, november 2008

1 Introduction

This report is a collection of preliminary results of the 1/12° model configuration NATL12. This configuration was used to perform a 27-year long interannual simulation (years from 1980 to 2006), during the summer of 2008. The NATL12 configuration has been created by MERCATOR-Ocean, and then updated within the DRAKKAR project (www.ifremer.fr/lpo/drakkar). The specificity of our configuration are the north and south boundaries (open climatological boundaries), the surface forcing (DFS4, Drakkar forcing set 4, Brodeau et al, 2008), and the bathymetry (opening of Faroe Bank Channel). A technical report describes the configuration in detail (Treguier 2008).

This numerical simulation (NATL12-BAMT20) can be compared to other DRAKKAR and MERCATOR simulations:

- another NATL12 experiment, 14-year long from 1980 to 1993, that was run in 2007 with closed boundaries (NATL12-BST41)
- the global 1/4 model experiment ORCA025-G70 (from 1958 to 2004) run by Jean Marc Molines at LEGI;
- another global 1/4 model experiment ORCA025-LIM-T09, run by MERCATOR (G. Garric) for the recent years (up to 2007).
- a number of 1/4 experiments over the same North-Atlantic/Nordic seas domain, run by Jean Marc Molines (NATL025 experiments), for a duration of 10 years (1980-1989).

In this report, we have chosen (arbitrarily) to use the time-mean fields over years 1996 to 2000 for the evaluation of the results. We also present some time series covering the duration of the experiment (1980-2006).

*Laboratoire de Physique des océans, CNRS-IFREMER-UBO, Plouzané, France

2 Sea Surface Anomaly

The variability of sea surface height is the easiest diagnostic of the main pathways of surface circulation and surface instabilities in eddy-resolving models. We consider the rms sea level anomaly from AVISO, averaged over years 1993-2004 (this time period was immediately available, but for further work it will be necessary to compare data and models over the same period). Resultats are shown for the whole basin as well as for the North-Eastern Atlantic and the subpolar gyre separately.

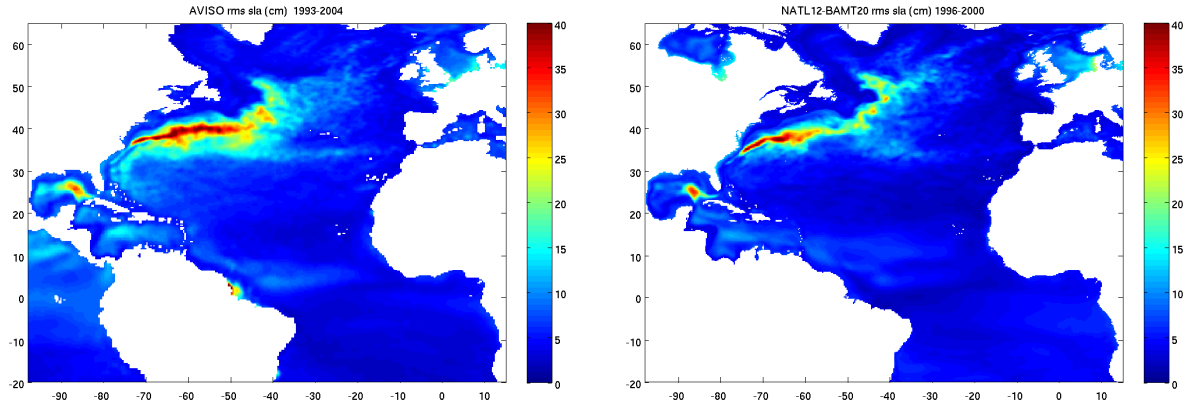

Figure 1: Rms sea level anomaly observed by altimetry (AVISO gridded product) compared with the model

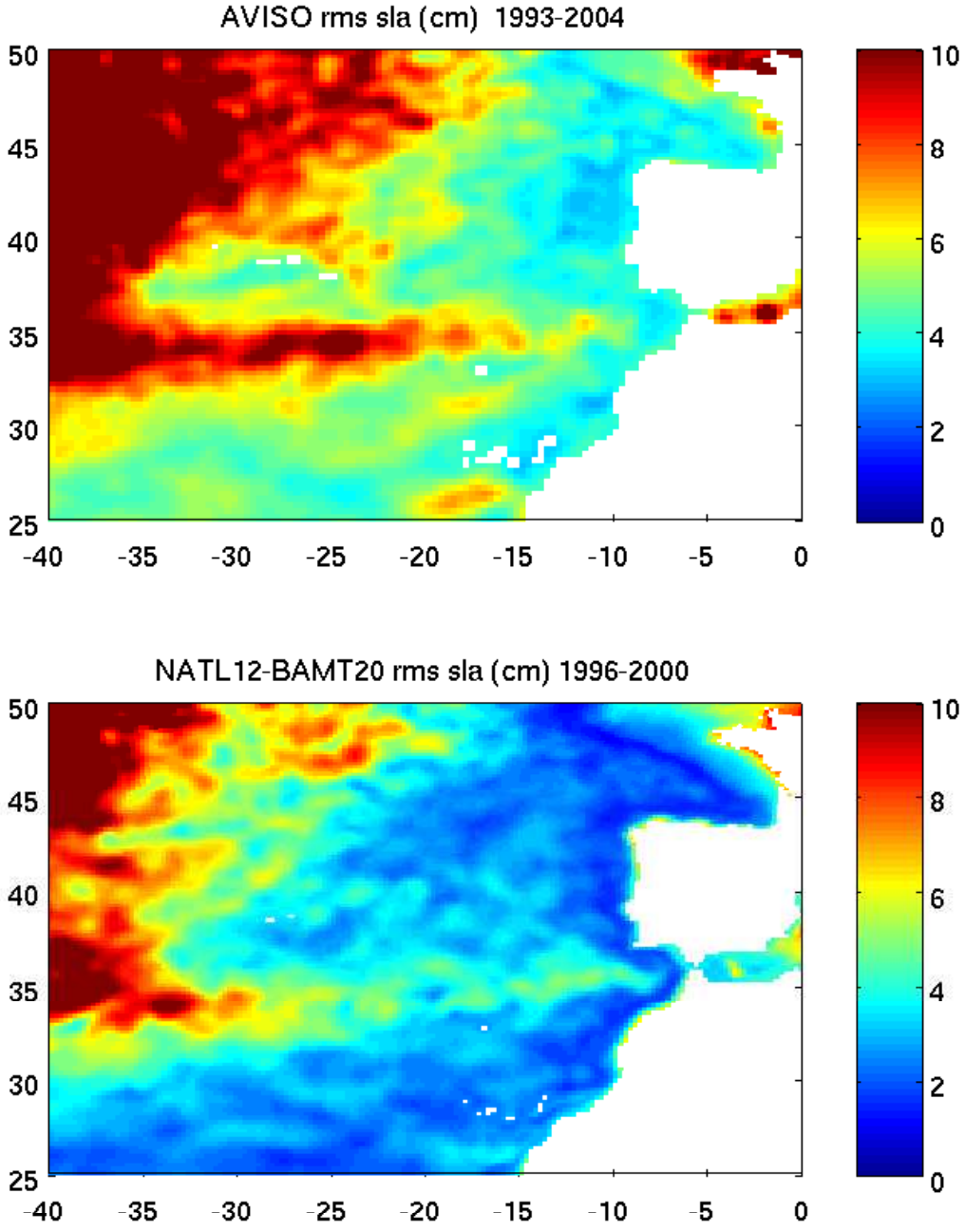

Figure 2: Rms sea level anomaly in the Eastern Atlantic, observed by altimetry and from the model.

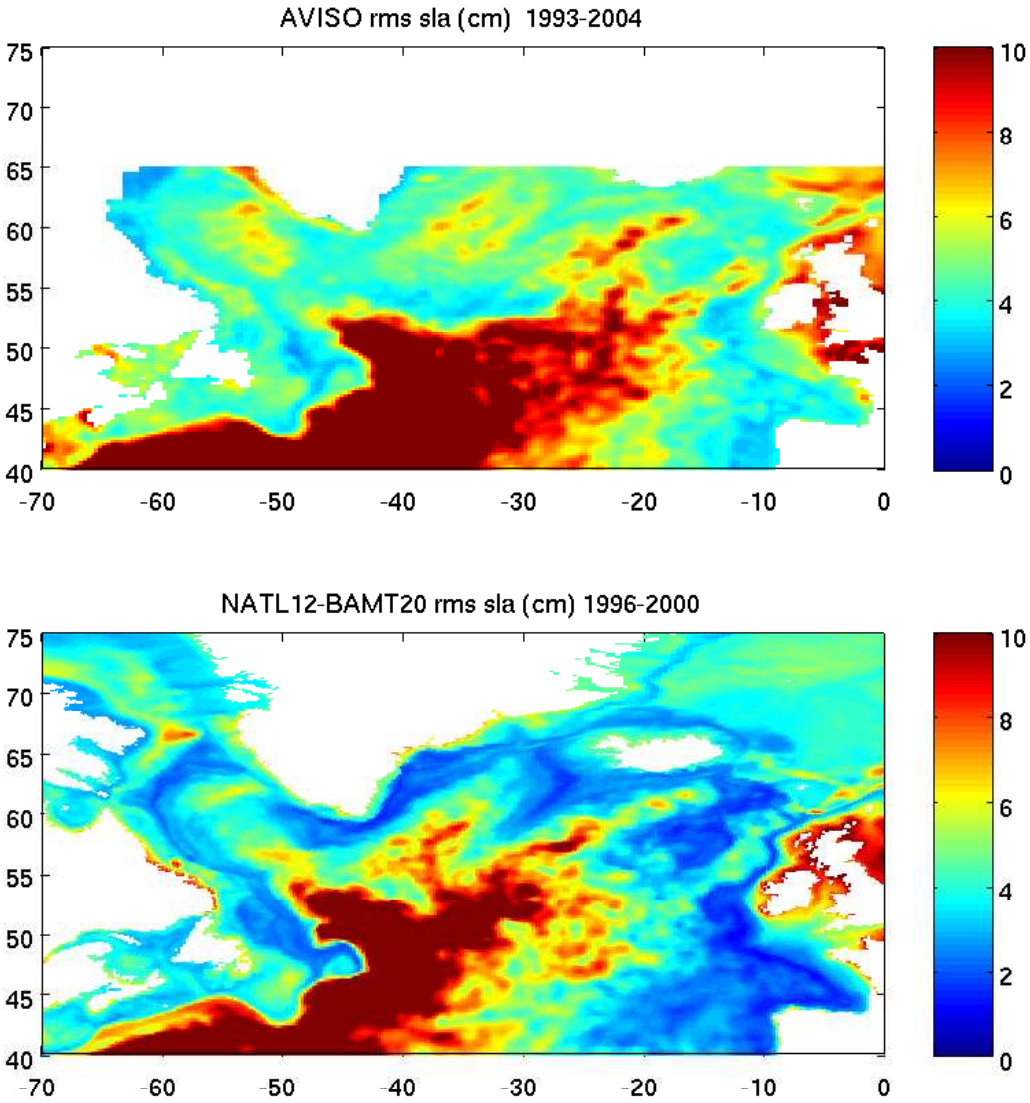

Figure 3: Rms sea level anomaly in the subpolar gyre, observed by altimetry and from the model.

3 Temperature and salinity drifts

The drift in temperature in NATL12-BAMT20 has the same decreasing tendency than ORCA025-G70 but with a larger amount. The 3D mean temperature decreases of 0.05°C in 27 years whereas the same amount is lost in 47 years of simulation in ORCA025-G70. There is a small increase centered in 1998, which is comparable to what happens in NATL025-G75 but with a weaker rise in the temperature. The drift in salinity goes the opposite way than those of ORCA025-G70 (Global) and NATL025-G75obc (Open Boundaries). However, it is quite similar with NATL025-G75 but with a smaller increase (0.004 in NATL12-BAMT20, 0.006 in NATL025-G75).

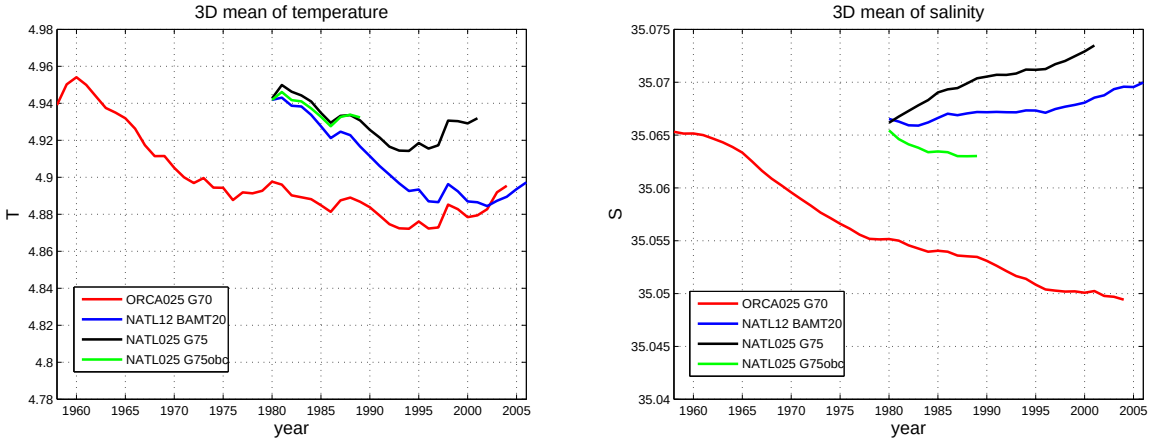

Figure 4: Temperature and salinity drift in models

4 Meridional Overturning and meridional heat transport

Overall, this simulation has a larger overturning than the NATL12-BST41 run (with closed boundaries and narrow Faroe Bank channel) and the ORCA025-G70 (global) run. The maximum MOC is 2-3 Sv larger in NATL12-BAMT20 than in NATL12-BST41 and 3-4 Sv larger than ORCA025-G70's maximum MOC in the atlantic basin. The MOC at 40°N shows a larger variability in the NATL12 simulations than in ORCA025-G70 and slightly stronger values. In addition, the MOC at 15°S in NATL12-BAMT20 is 1.5 Sv stronger than ORCA025-G70 and 4-5 Sv stronger than NATL12-BST41. It is interesting to analyse the overturning at 15°S, not far from the southern boundary. In the experiment with closed boundaries (NATL12-BST41) the overturning had a tendency to increase over the course of the simulation, and we thought it was an artefact. However, here we find the same tendency (figure 9). This increase thus seems driven by the dynamics of the basin itself, and happens at high resolution (we do not find the same tendency in ORCA025-G70). What's more, we find out that the MOC at the open boundary shows an increase of 0.1 Sv/year.

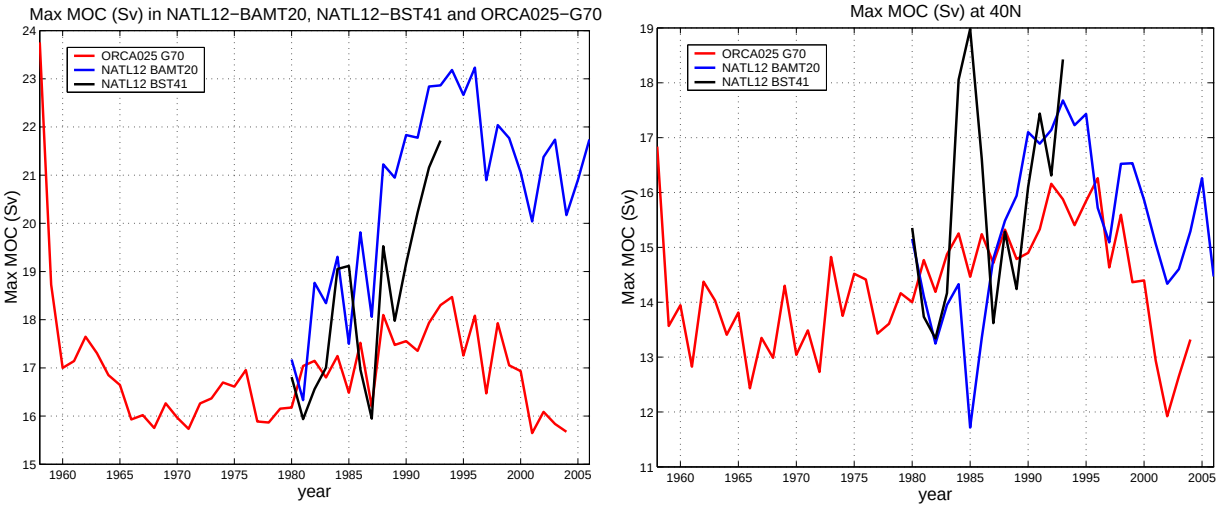

Figure 5: Comparison of maximum MOC (*left*) and maximum MOC at 40°N(*right*) in NATL12-BAMT20, NATL12-BST41 and ORCA025-G70

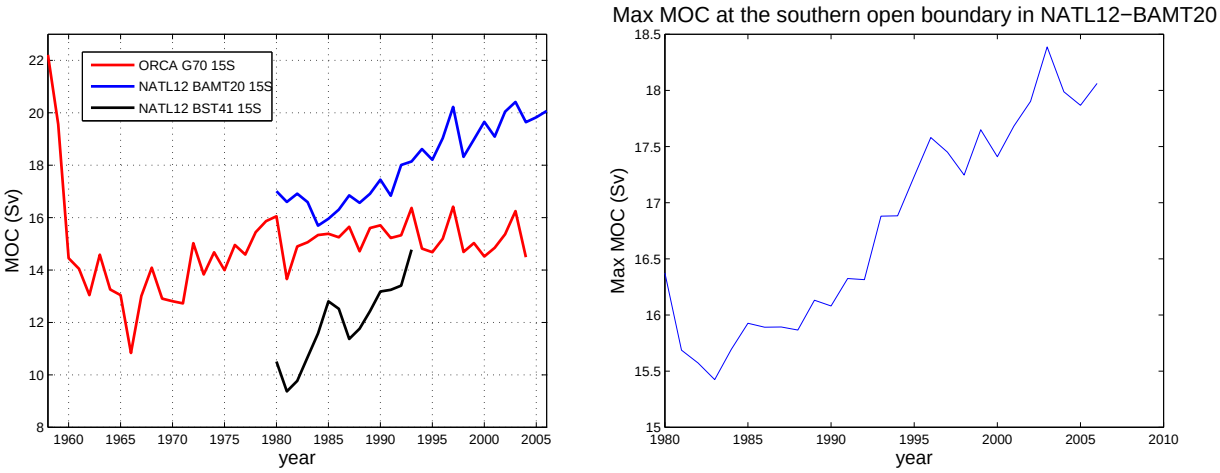

Figure 6: *left panel :* Comparison between NATL12-BAMT20, NATL12-BST41 and ORCA025-G70 at 15°S . *right panel :* Focus at the southern open boundary. It has an increasing of 0.1 Sv/year.

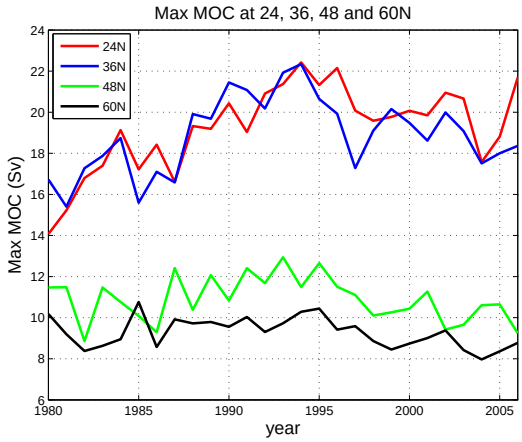

Figure 7: Maximum MOC in NATL12-BAMT20 at 24°N, 36°N, 48°N and 60°N

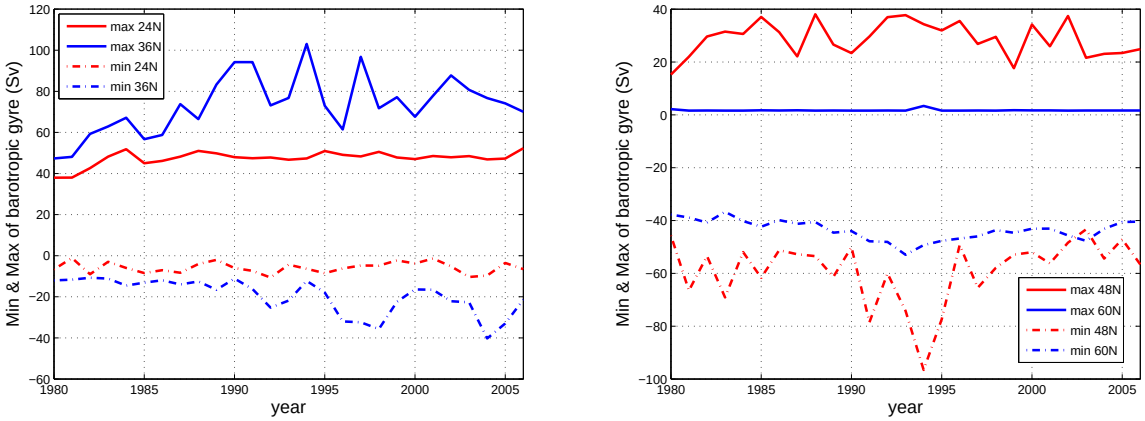

Figure 8: Time series of Minima and Maxima of barotropic gyre at 24°N, 36°N(*left panel*) , 48°N and 60°N(*right panel*)

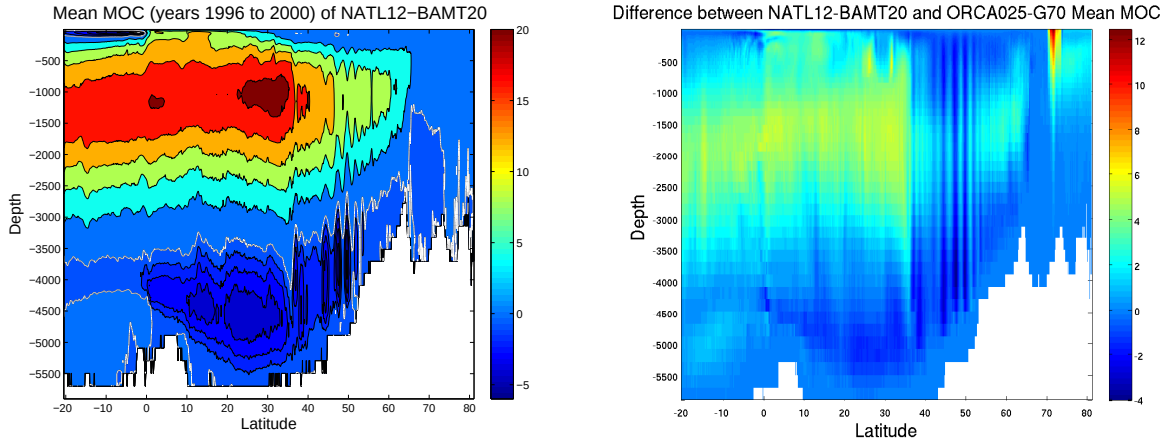

Figure 9: *left panel :* Mean of the Meridional Overturning cell (z-coordinates) from years 1996 to 2000. *right panel :* Difference NATL12-BAMT20 minus ORCA025-G70 (same years)

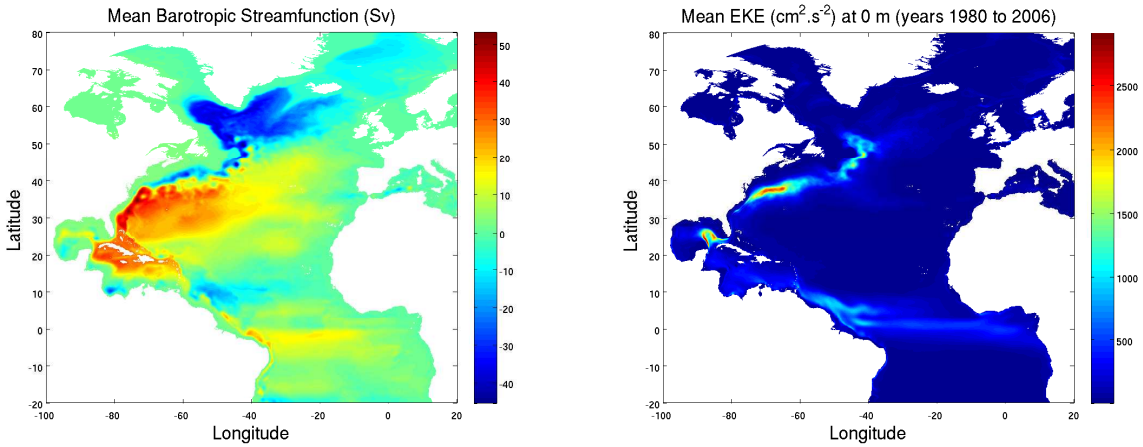

Figure 10: *left panel :* Mean Barotropic Streamfunction from years 1980 to 2006. *right panel :* Mean EKE at 3m.

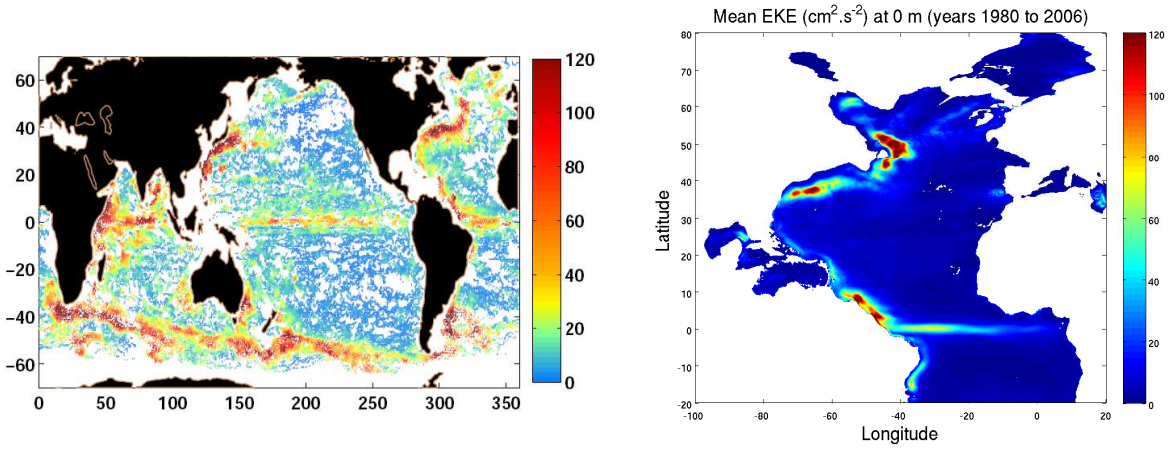

Figure 11: *left panel :* EKE ($cm^2.s^{-2}$ at 1000 m from Cabanes et al. 2008 *right panel :* Mean EKE at 1040m in NATL12-BAMT20 (maximum reaches 250 $cm^2.s^{-2}$)

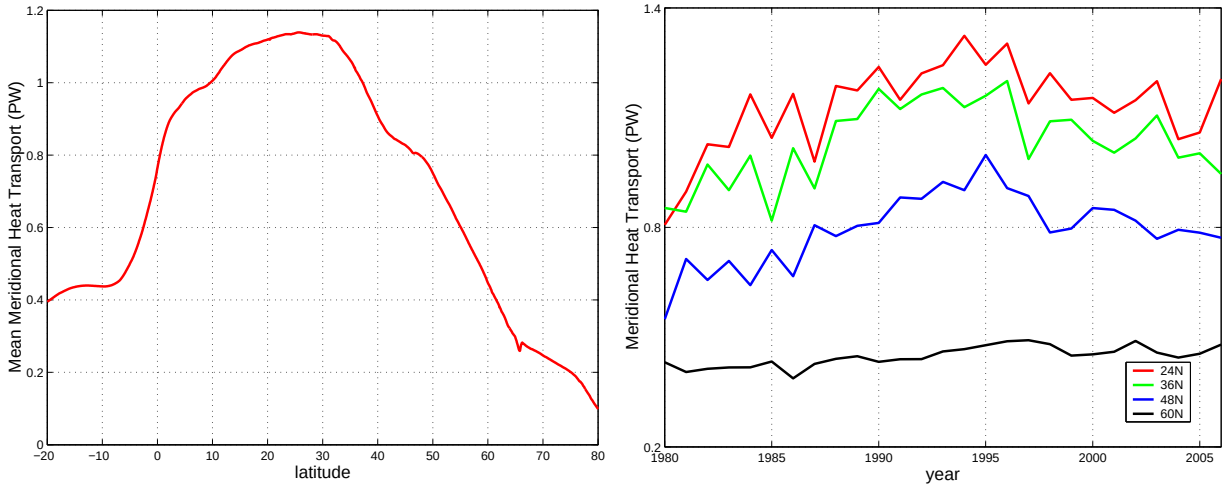

Figure 12: *left panel :* Mean Meridional Heat Transport (years 1980 to 2006). *right panel :* Time series of Heat Transport at 24°N, 36°N, 48°N and 60°N

5 Equatorial Under Current

The strength of the equatorial undercurrent (EUC) is very dependent on subgrid scale parameterizations. In the CLIPPER 1/6° model the EUC was too strong, and a horizontal Laplacian viscosity was added between 2°S and 2°N to solve the problem (Arhan et al, 2006). On the other hand, the new momentum advection scheme implemented in NEMO (Barnier et al, 2006) tends to slow down the Equatorial Undercurrent. When we implemented NATL12 at IDRIS in 2007 we first ran two years with no laplacian viscosity, but the EUC was too strong and we added again Laplacian viscosity with a coefficient of 250 $m^2.s^{-1}$. This value was found too strong, so for the present experiment we use a Laplacian viscosity of 125 $m^2.s^{-1}$. A comparison with ADCP observations (Arhan et al, 2006) is shown in Fig.13. The mean velocity seems satisfactory (perhaps still a bit too slow?).

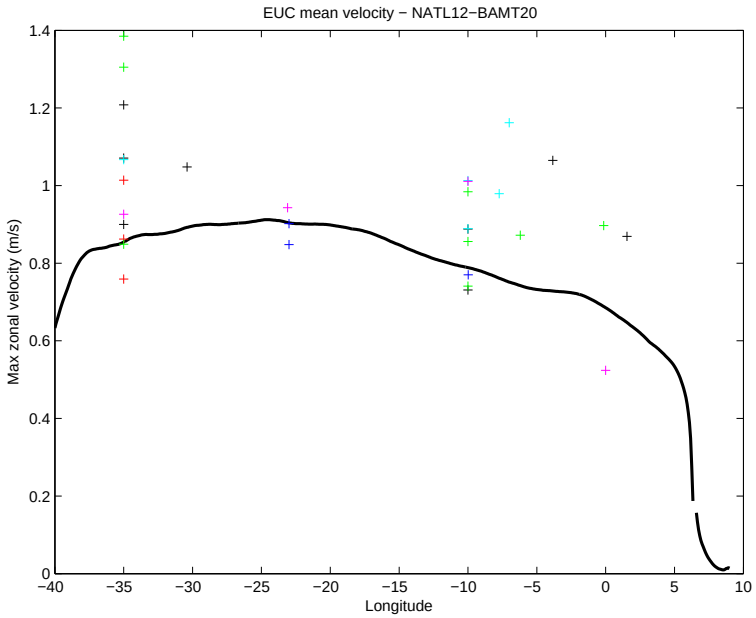

Figure 13: Maximum zonal velocity at the equator. Data points are ADCP instantaneous measurements at differents months/years from Arhan et al (2006).

6 Mediterranean Waters

The representation of the Mediterranean water ouflow and spreading into the Atlantic is an unsolved problem in models, even at 1/12° resolution. A satisfactory solution has been found for the global 1/4° model by using a combination of topography tuning (creating an artifical channel to allow the Med Water to sink downstream of Gibraltar, rather than turn north along the slope) and relaxation to climatology. In the NATL12-BST41 experiment, nothing was done and the Med outflow ended up being to high in the water column (Fig 21). In NATL12-BAMT20, a combination of no-slip boundary condition and topography editing allow the outflow to reach the right depth. It is however too warm and too saline (Fig. 20), leading to a large drift of properties around 1000-1500 m depth.

Regarding the flow in Gibraltar Strait, there is a net flow of 0.03 Sv into the Mediterranean to compensate for the evaporation. The average exchange flow (westward volume transport is 0.955 Sv for years 1996-2000. Estimates for the deep outflow varies between 0.67 and 0.97 so the model is in the upper range but the transport is not unrealistic. Fig. 14 shows a time-series of transport in density classes as well as the total westward transport. It shows a good stability of the transport during the course of the simulation.

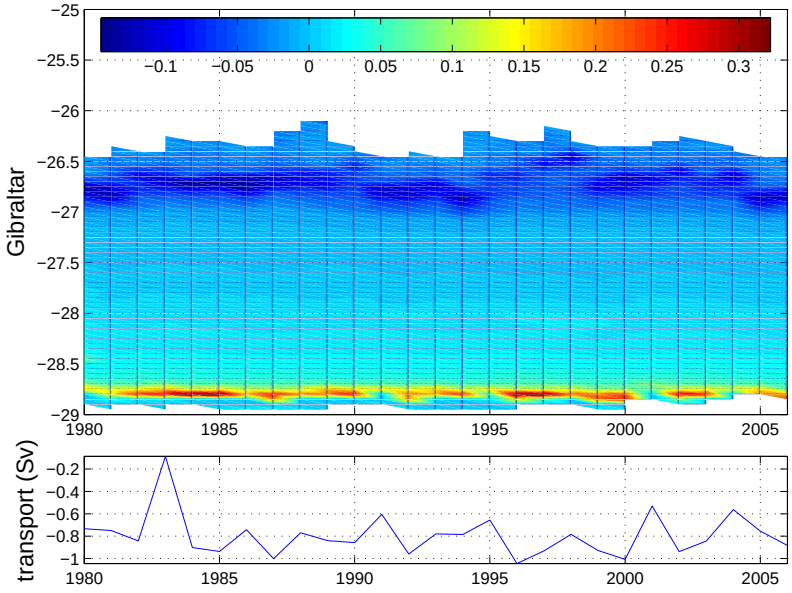

Figure 14: Time serie of Transport in sigma classes (top) and time serie of integrated Transport (bottom)

The path of the Med water ouflow downstream of Gibraltar is represented by a map taken from Johnson et al (1994), Fig.15. The map indicate in grey locations where the proportion of Med Water is larger than 50%. The distribution of Med water percentage closely follows the salinity field, so that it is possible to draw a map of model maximum salinity with contours corresponding to the figure. The salinity contours 36, 36.3, 36.6, 36.9, 37.15, 37.4, 37.7, 38., 38.5, correspond to fractions 0.1, 0.2, 0.3, 0.4, 0.5, 0.6, 0.7, 0.8 and 1. The model results as

shown in fig.16. The plume reaches the 1000 m isobath at a longitude slightly west of 7°W, which is something difficult to reproduce in models at that resolution (especially z-coordinate models).

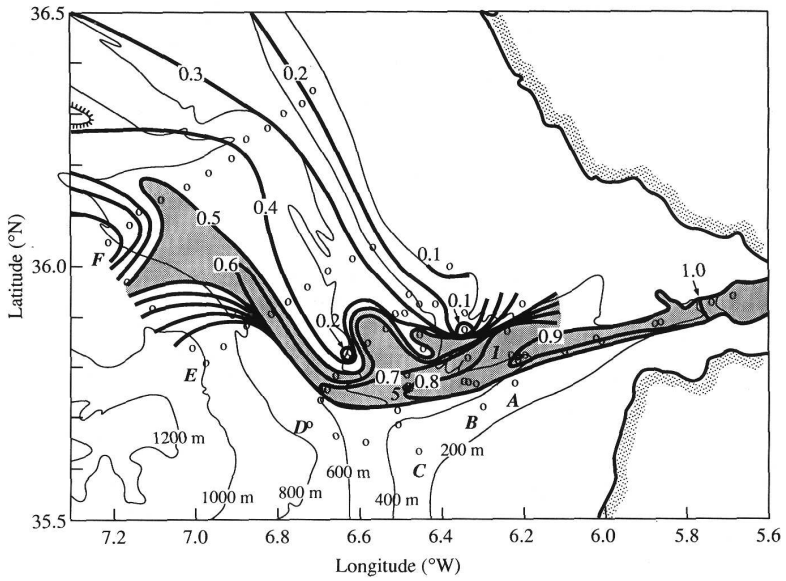

Figure 15: Contours of maximum Mediterranean water fraction at 0.1 intervals showing the Mediterranean outflow plume (reproduced from Johnson et al, 1994, their Fig.1). MW fraction larger than 0.5 is stippled.

Let us consider more precisely how the maximum salinity as a function of longitude. The decay in the model matches observed values taken from the litterature (Fig.17).

Despite this apparent agreement close to the source, the input of salt into the Atlantic is obviously too large, because the salinity field shows a large drift. Figures 18 and 18 show the horizontal spreading of salt due to the Med Water. Comparison between model's contours (black contours) and climatology (white contours) indicates that the model can be up to 0.5 PSU saltier, especially at 1040 and 1260 meters deep. Temperature and salinity profiles (computed in the (10W-13W,35N-40N) region) confirm that the outflow is now located at the right depth but is 0.3 PSU too salty and 1 deg too warm compared to climatology and ORCA025-G70 run. The transport in this area is 0.8 to 1 Sv (Fig 21), which is close to the values obtained in ORCA025-G70. We also compared with data from the SEMANE 2002 section at 8.2°W (figures 22). The salinity in the model in july 2002 is 0.3 PSU saltier than the observations. However, if we compare the observations with the mean salinity in the model from 1996 to 2000, we get only 0.1 PSU difference. Is this means that we have an increase of the salinity downstream of the Gibraltar strait with time or simply that the model didn't fit the observations in july 2001 but the mean salinity at 8.2°W is ok. Fig 23 shows that the upper and lower core of the Med Water ouflow are well positioned at 750 and 1250 meters deep.

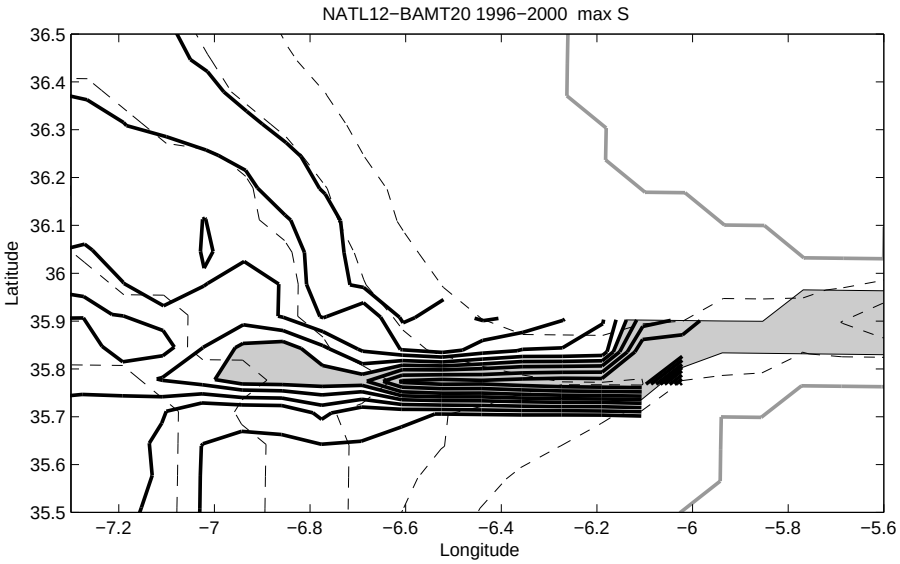

Figure 16: Maximum salinity over depth in the NATL12 model downstream of Gibraltar. Salinities greater than 37.15 are shaded. contours are 36, 36.3, 36.6, 36.9, 37.15, 37.4, 37.7, 38., and 38.5 for salinity. Isobaths 200 to 1000 m by 200 m are indicated.

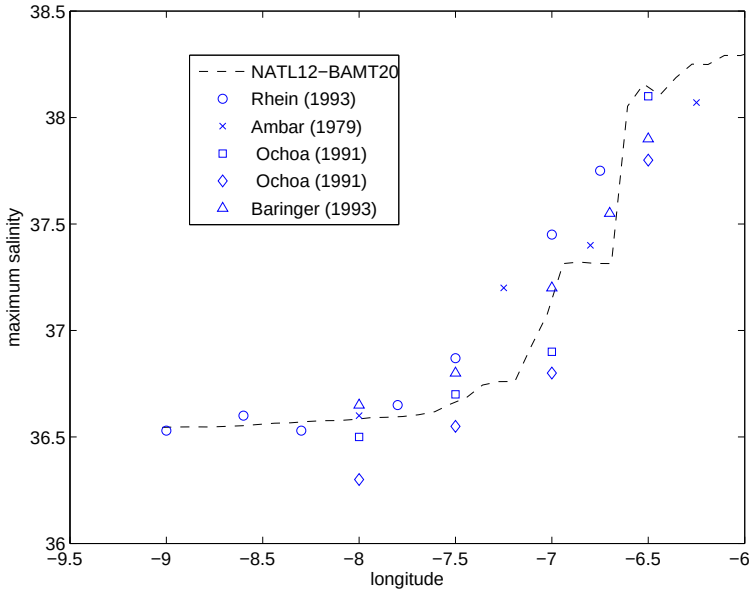

Figure 17: Maximum salinity (maximum over depth below 155 m and latitude) in the Gulf of Cadiz, downstream of Gibraltar Strait. Observations from the litterature are shown for comparison (see list of references).

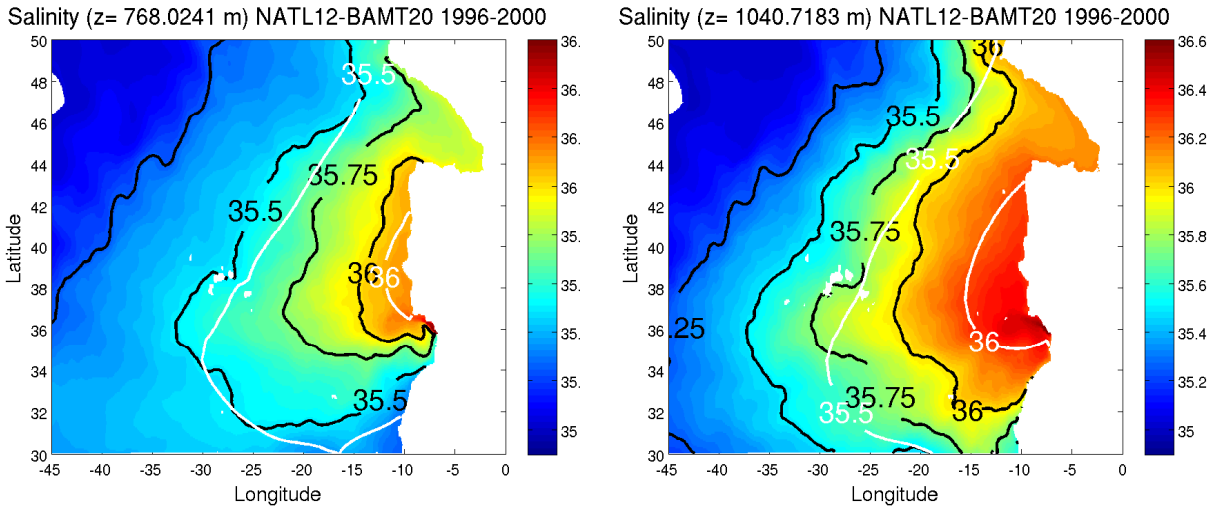

Figure 18: Interannual Mean of salinity from 1996 to 2000 in NATL12-BAMT20 at $z = 768$ m (*left*) and $z = 1040$ m (*right*). For comparison, two contours of Levitus (35.5 ans 36) are plotted in white.

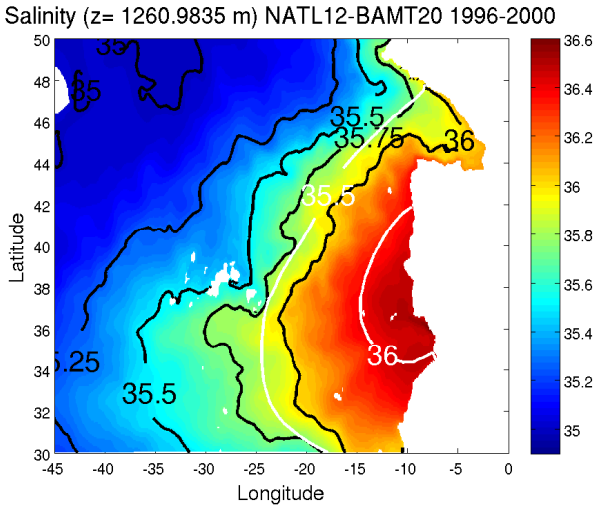

Figure 19: Interannual Mean of salinity from 1996 to 2000 in NATL12-BAMT20 at $z = 1260$ m. For comparison, two contours of Levitus (35.5 ans 36) are plotted in white.

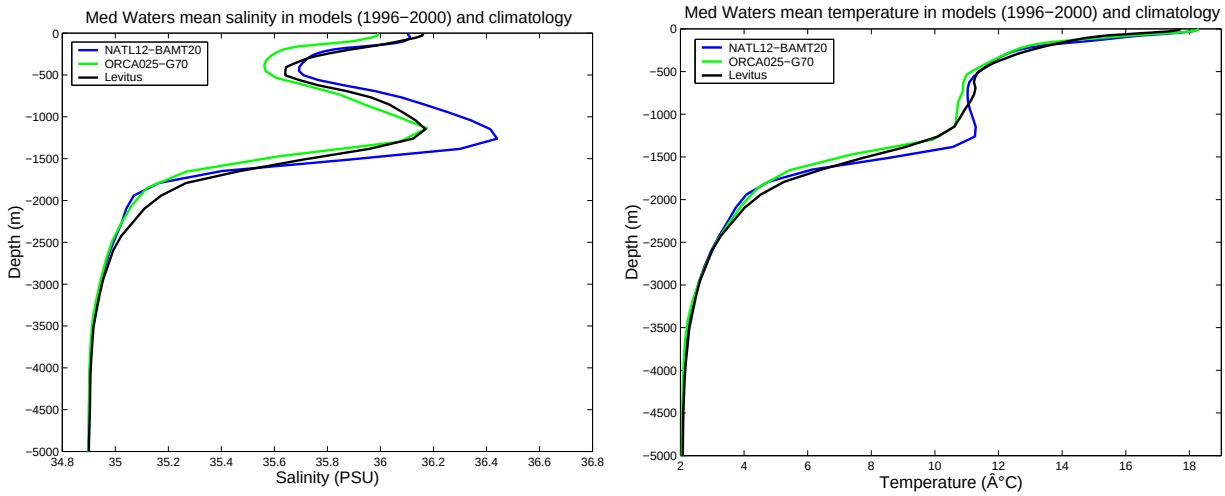

Figure 20: vertical profiles of mean salinity (left) and mean temperature (right) in models (years 1996-2000) and climatology.

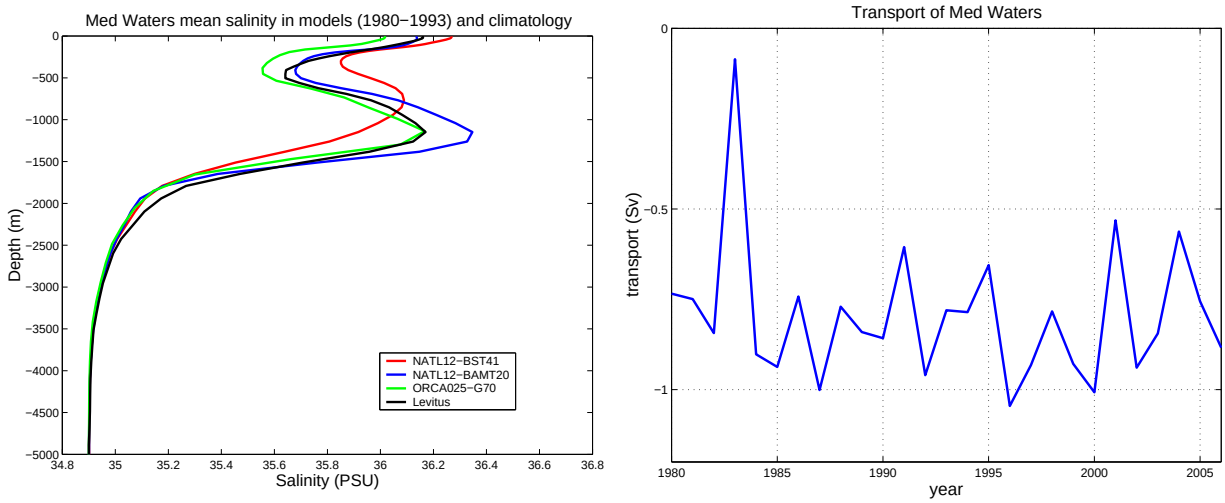

Figure 21: left : Salinity profile (years 1980-1993). Notice how BST41 is less salty and not deep enough. right : time serie of transport in NATL12-BAMT20

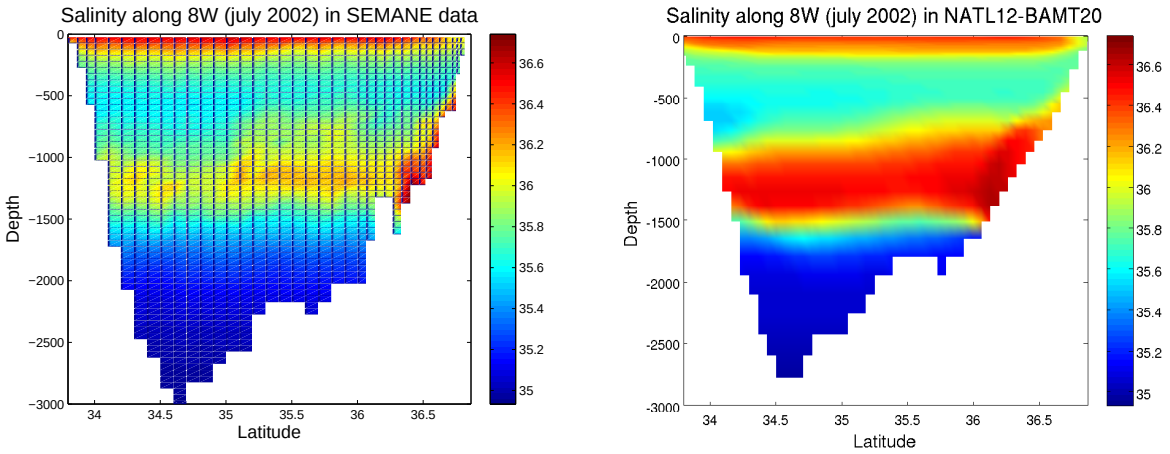

Figure 22: Salinity (july 2001) at 8.20 °W in NATL12-BAMT20 (*left*) and SEMANE 2002 Data (*right*)

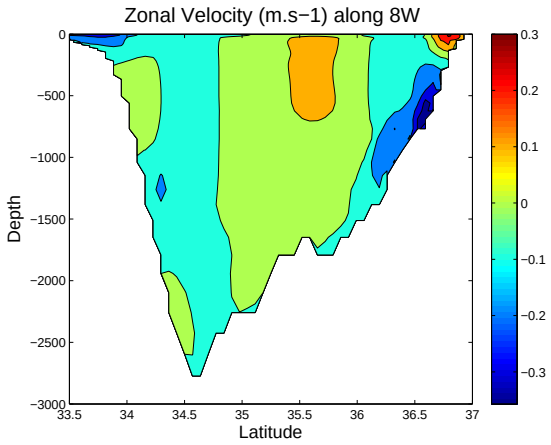

Figure 23: Zonal velocity in the model through SEMANE in 2001

7 Mixed layer depth

The mixed layer depth is compared to that deduced from climatological data (based on ARGO drifters with criterion $\rho < 0.03$, [de Boyer Montegut et al.(2004)]) The model criterion is $\rho < 0.01$. The agreement is fairly good in september as the mixed layer depth is 60 meters in both cases (Fig 25). With a mixed layer depth that reaches 3000 meters in march, the convection is too deep in the model (Fig 24).

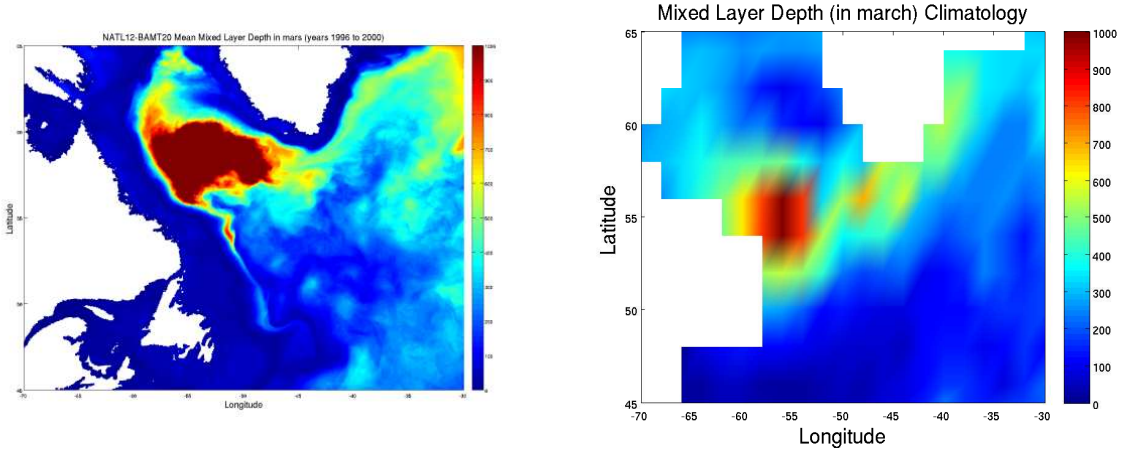

Figure 24: Interannual Mean of Mixed Layer Depth in th Labrador Sea in NATL12-BAMT20 (left) compared to Clement de Boyer Montegut climatology (right) in march 1996-2000

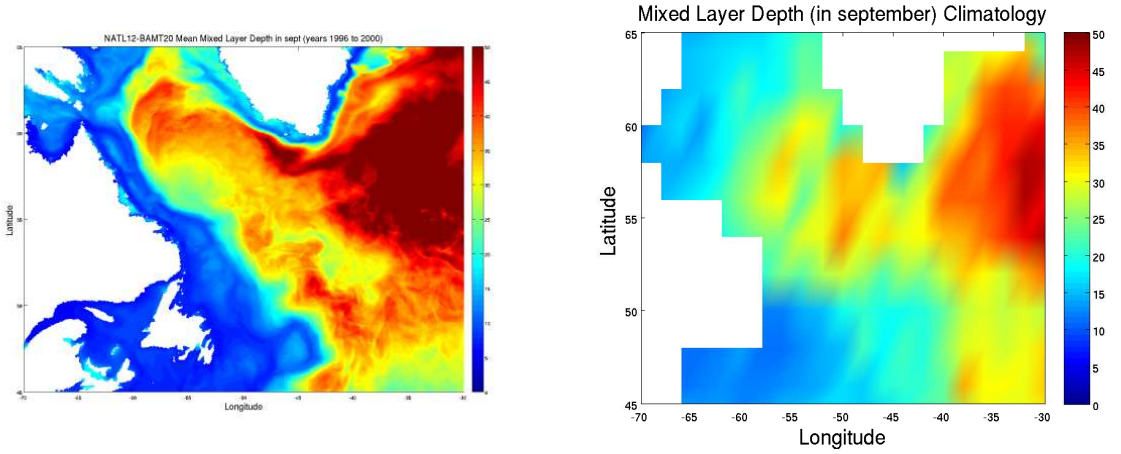

Figure 25: Interannual Mean of Mixed Layer Depth in th Labrador Sea in NATL12-BAMT20 (left) compared to Clement de Boyer Montegut climatology (right) in september 1996-2000

8 Nordic seas overflows

The use of no-slip boundary conditions in the overflow region, as well as the deepening of Faroe Bank channel, has led to a significant improvement compared with other Drakkar configurations, but the model still has problems as shown by a comparison of the bottom density with observations (Fig.26. The Denmark Strait overflow plume appears clearly, but the waters at the bottom of the Irminger sea (presumably supplied by the overflows, after recirculation and mixing?) are too light in the model. the situation is worse in the Iceland basin, where the Faroe Bank channel outflow fails to supply dense water. Note that although the transport through Faroe Bank channel is realistic, the temperature is not (the model temperature is too high) and therefore the mean density of the overflow is probably too light.

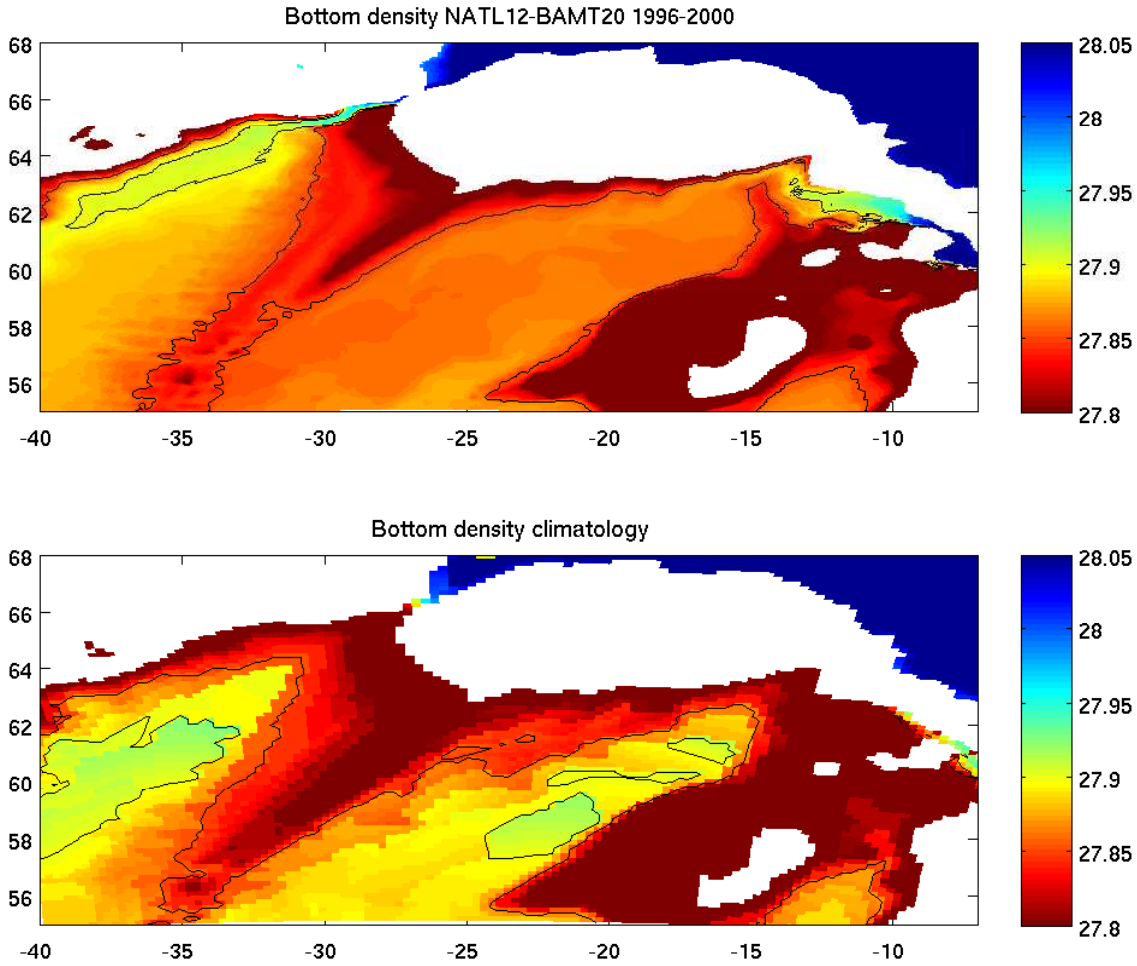

Figure 26: Bottom density (σ_0). top: model; bottom: Levitus climatology.

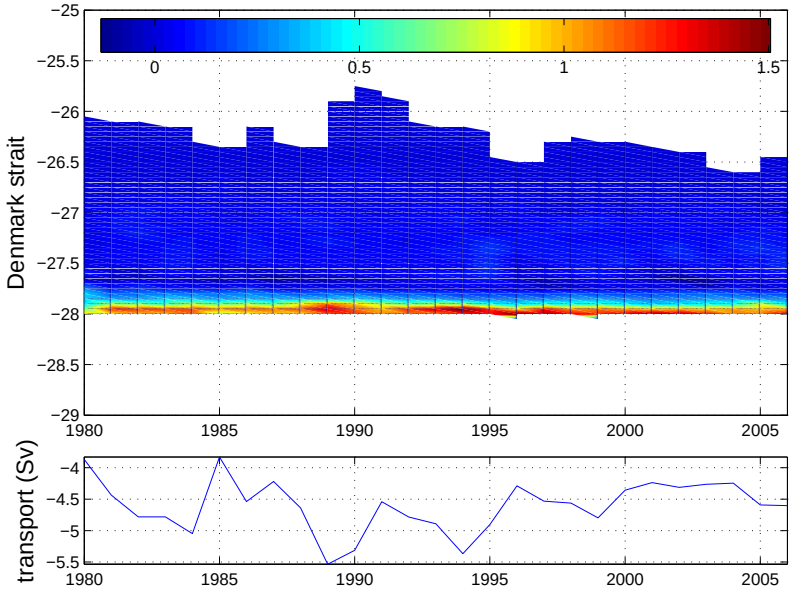

Figure 27: Time serie of Transport in sigma classes (top) and time serie of integrated Transport (bottom)

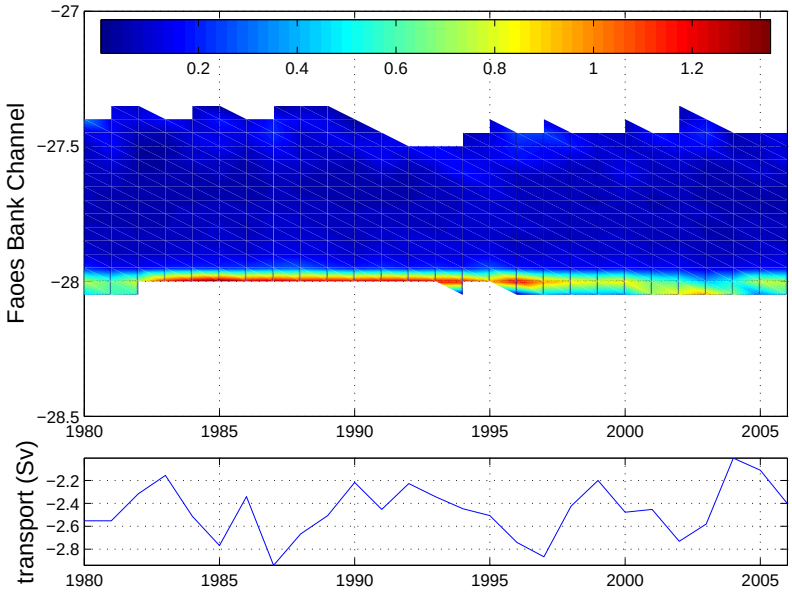

Figure 28: Time serie of Transport in sigma classes (top) and time serie of integrated Transport (bottom)

9 Water mass properties in the subpolar gyre

One of the biggest challenges for high resolution models is the maintain the low salinity of the Labrador Sea water in the subpolar gyre (Treguier et al, 2005). Figure 29 shows that the salinity in the Labrador Sea grows with time. This is probably due to the salt which is spread by the Med Water. Figures 30 and 31 indicate that the model is too salty in the Labrador sea, especially near the surface.

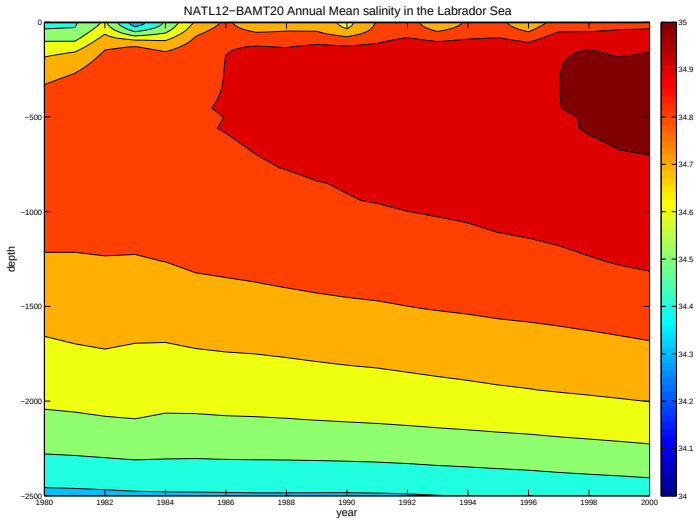

Figure 29: Salinity Profile in the Labrador sea (55W-47W,55N-58N) in time-depth coordinates

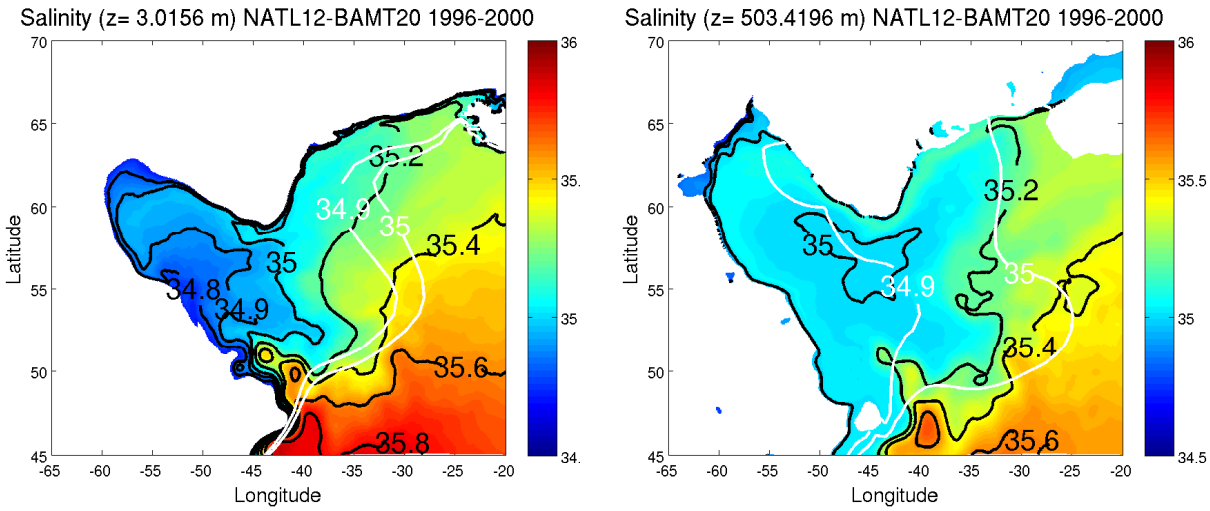

Figure 30: Interannual Mean of salinity from 1996 to 2000 in NATL12-BAMT20 at $z = 3$ m (*left*) and $z = 500$ m (*right*). For comparison, two contours of Levitus (34.9 ans 35) are plotted in white.

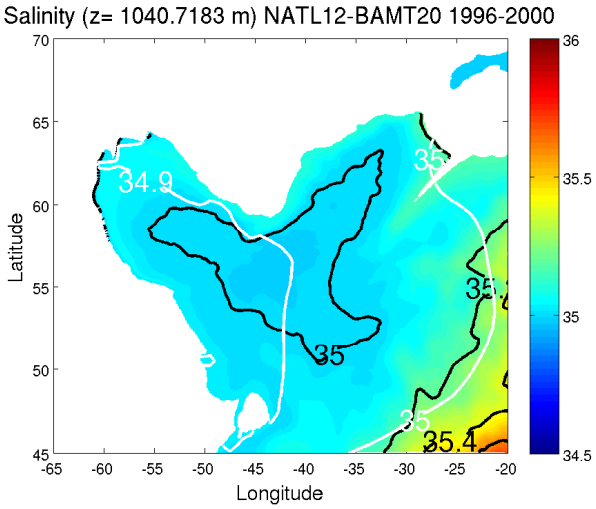

Figure 31: Interannual Mean of salinity from 1996 to 2000 in NATL12-BAMT20 at $z = 1000$ m. For comparison, two contours of Levitus (34.9 ans 35) are plotted in white.

10 Comparison with OVIDE data

Ovide is a cruise from portugal to greenland repeated every two years. We compare model's salinity, potential temperature and density anomaly referenced at 1000 m with those obtained during the 2002, 2004 and 2006 cruises (L'herminier et al., 2007 & Gourcuff, 2008).

10.1 Ovide 2002

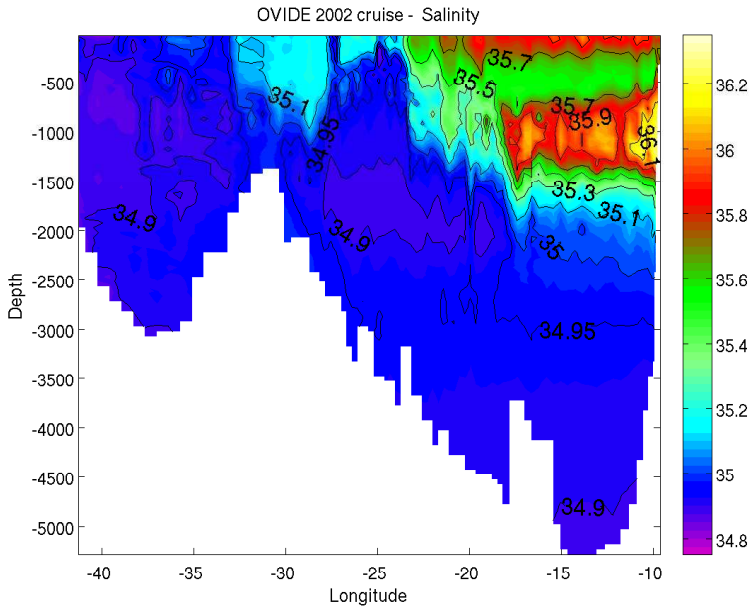

Figure 32: Salinity in OVIDE 2002 section

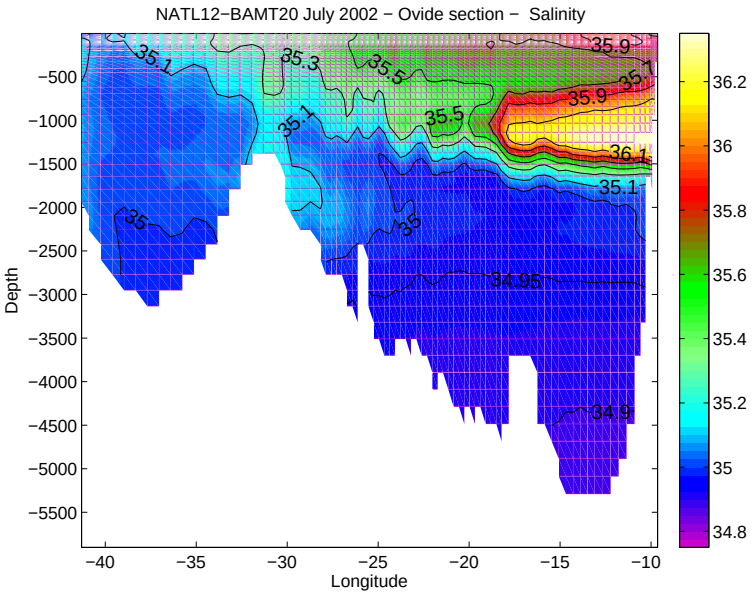

Figure 33: Salinity in NATL12-BAMT20 along OVIDE 2002

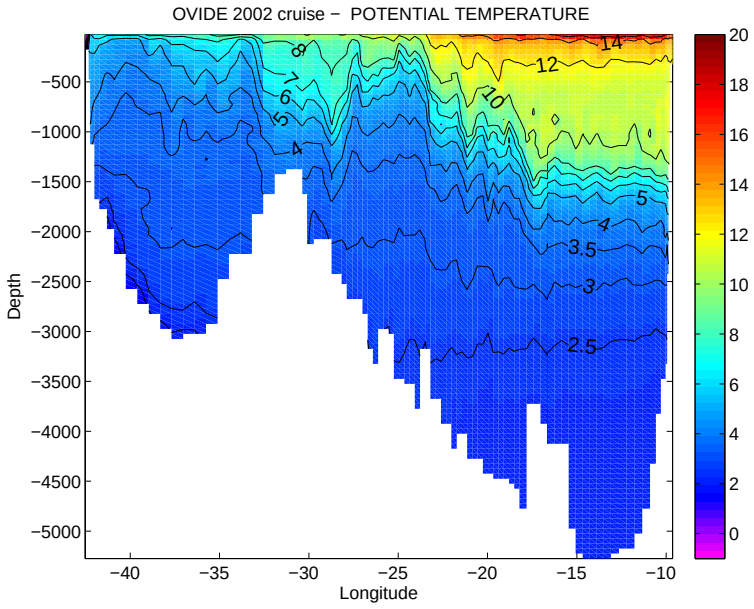

Figure 34: Potential temperature in OVIDE 2002 section

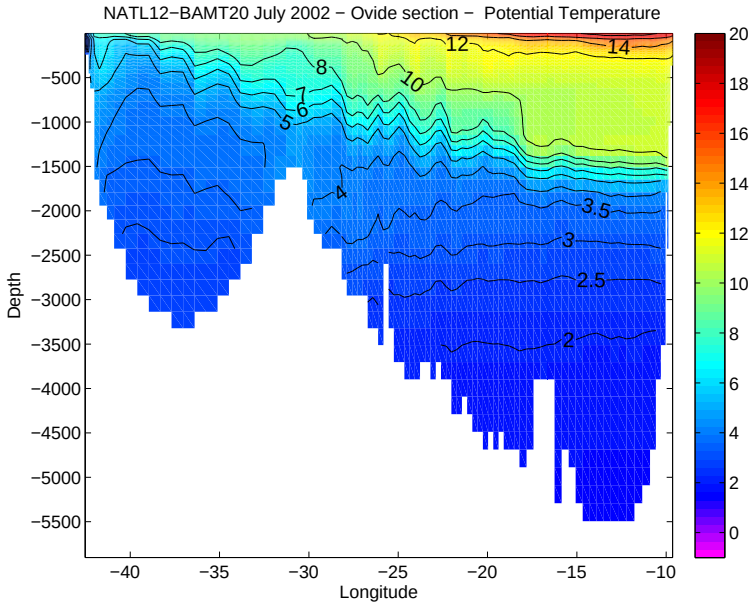

Figure 35: Potential temperature in NATL12-BAMT20 along OVIDE 2002

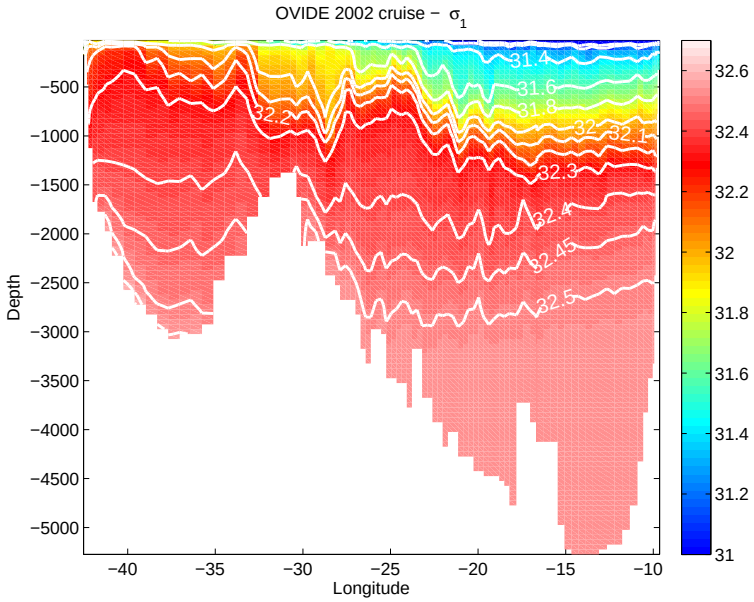

Figure 36: Density anomaly referenced at 1000 m in OVIDE 2002 section

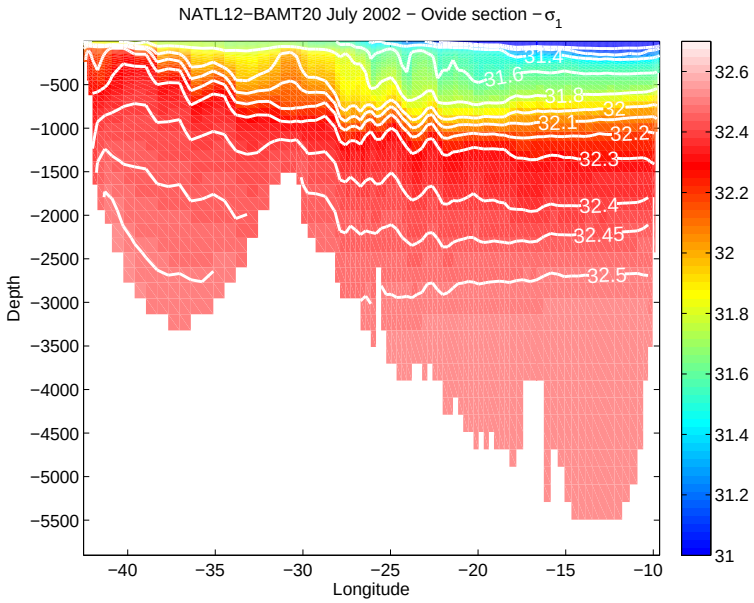

Figure 37: Density anomaly referenced at 1000 m in NATL12-BAMT20 along OVIDE 2002

10.2 Ovide 2004

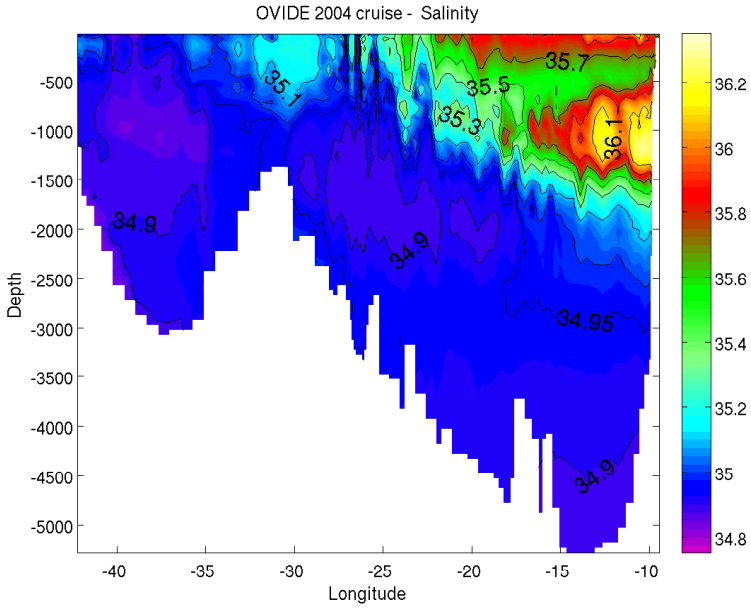

Figure 38: Salinity in OVIDE 2004 section

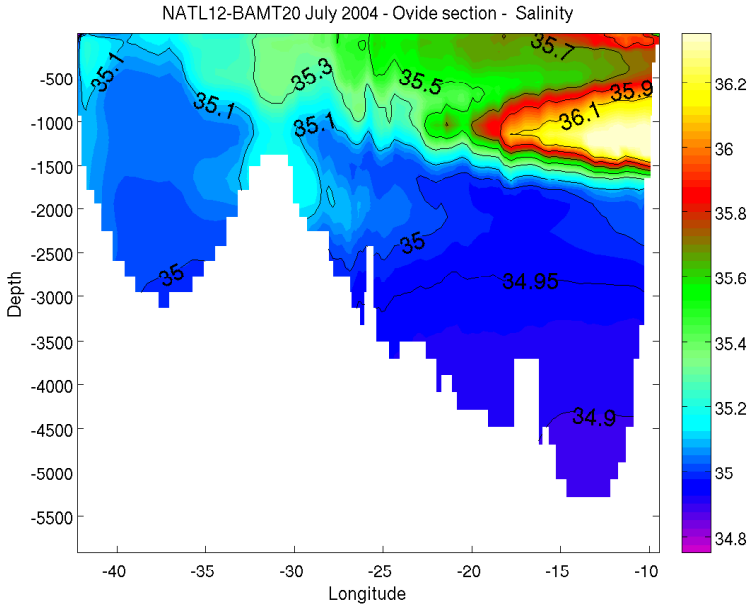

Figure 39: Salinity in NATL12-BAMT20 along OVIDE 2004

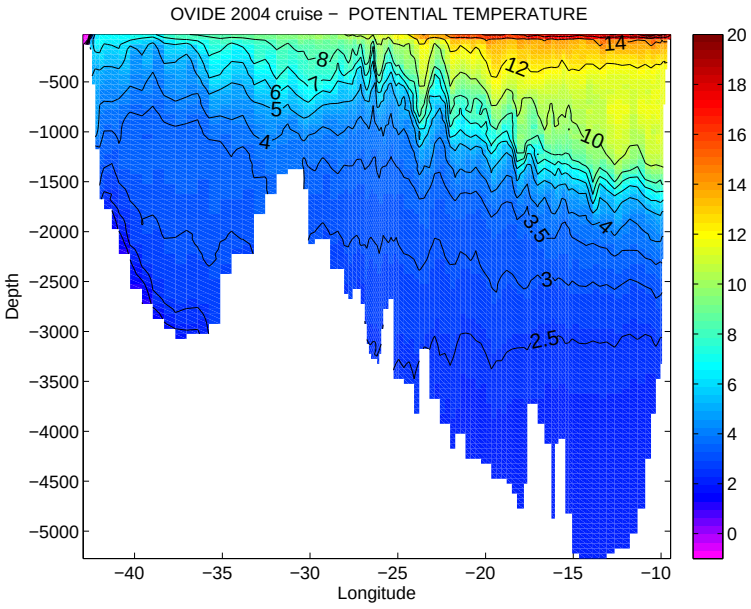

Figure 40: Potential temperature in OVIDE 2004 section

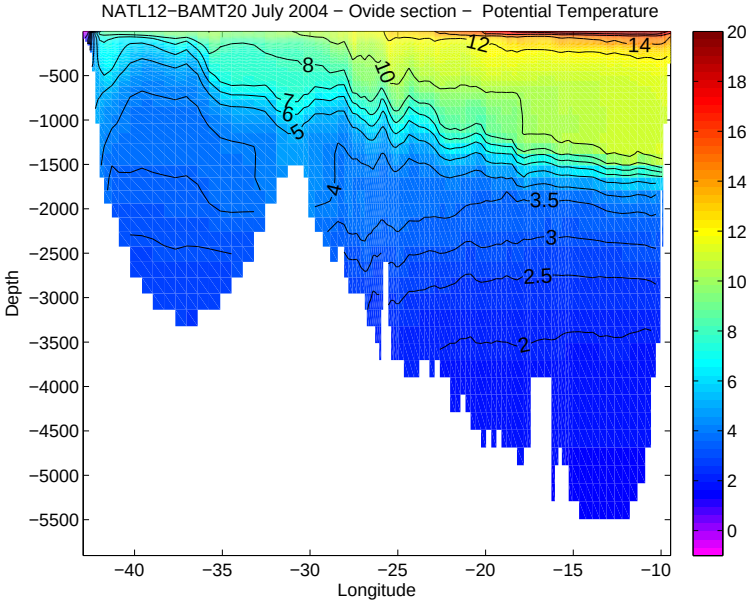

Figure 41: Potential temperature in NATL12-BAMT20 along OVIDE 2004

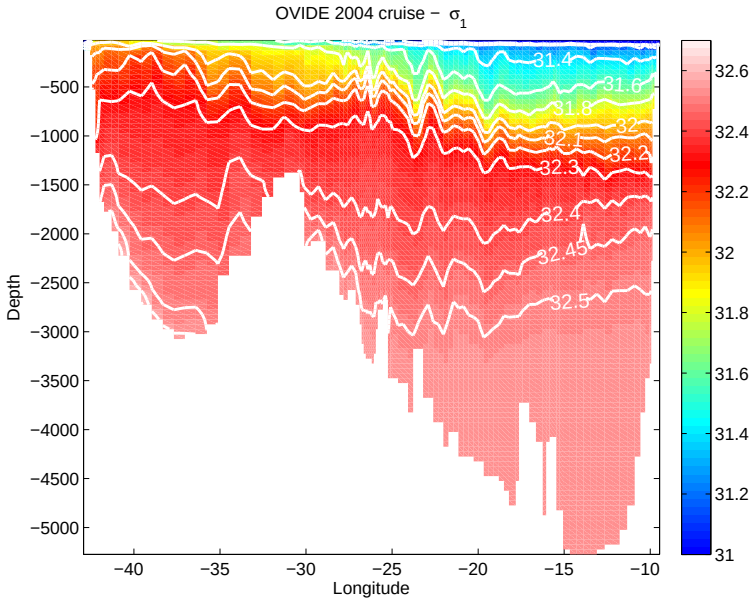

Figure 42: Density anomaly referenced at 1000 m in OVIDE 2004 section

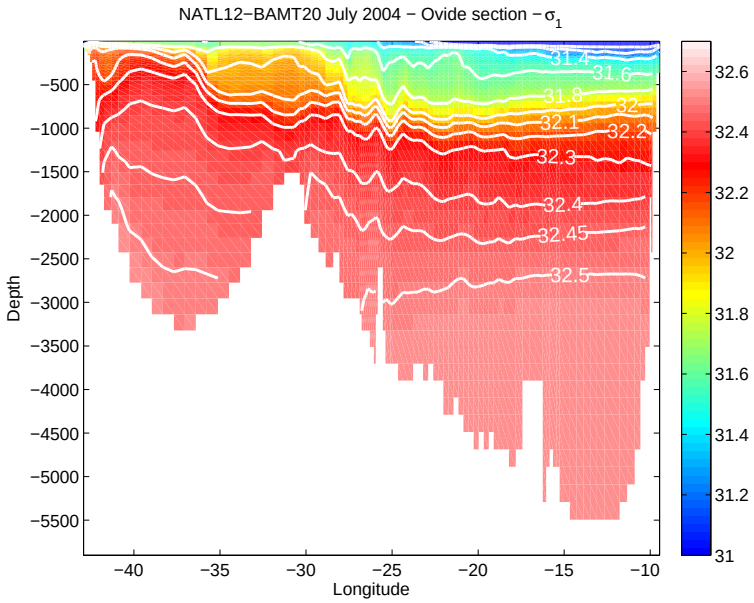

Figure 43: Density anomaly referenced at 1000 m in NATL12-BAMT20 along OVIDE 2004

10.3 Ovide 2006

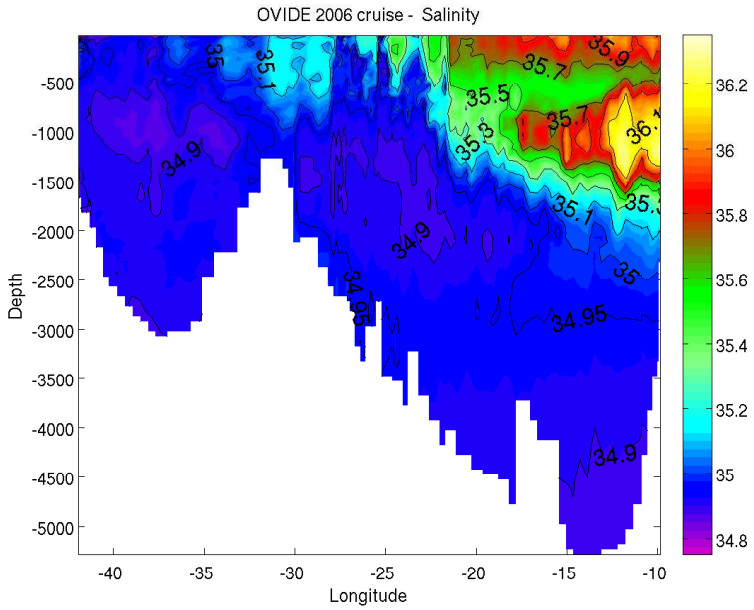

Figure 44: Salinity in OVIDE 2006 section

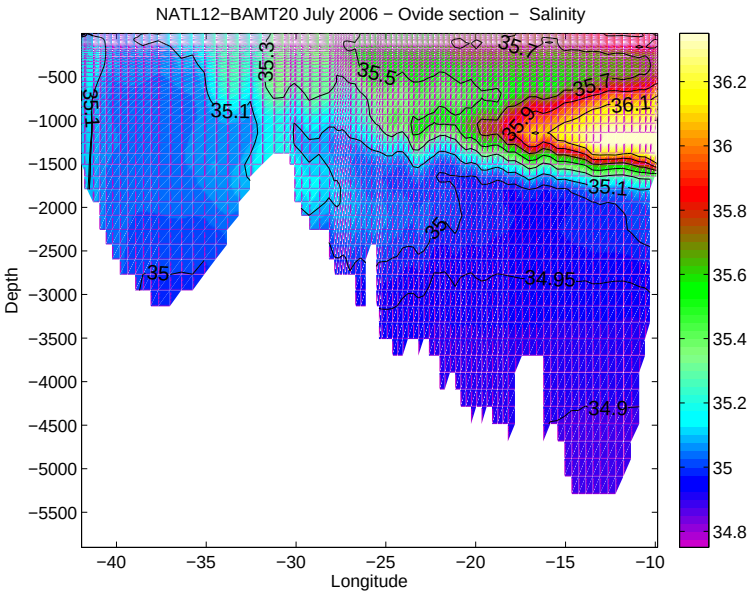

Figure 45: Salinity in NATL12-BAMT20 along OVIDE 2006

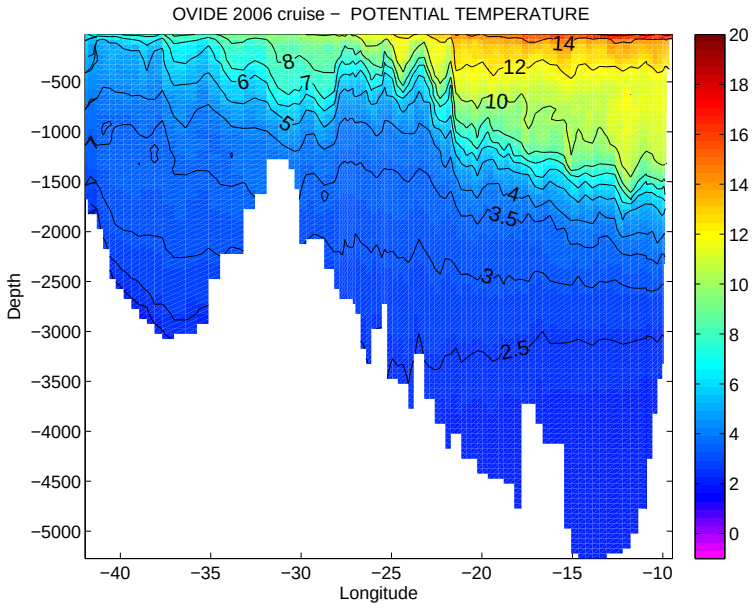

Figure 46: Potential temperature in OVIDE 2006 section

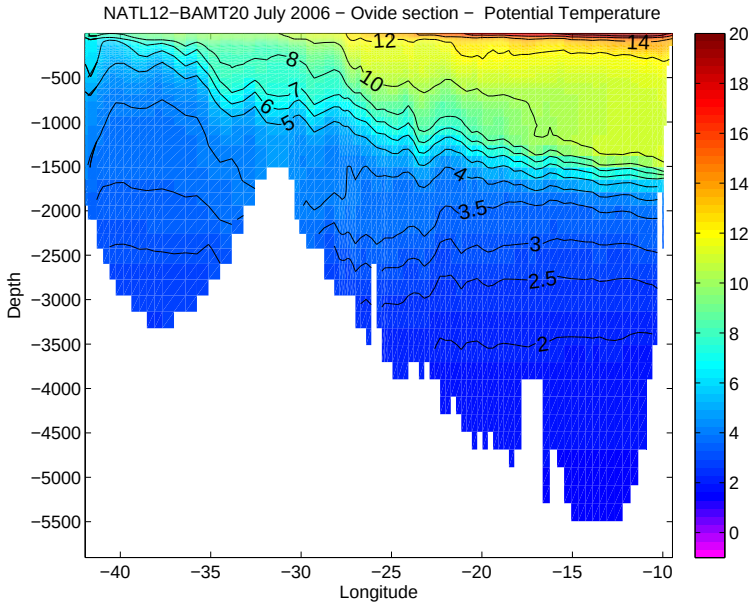

Figure 47: Potential temperature in NATL12-BAMT20 along OVIDE 2006

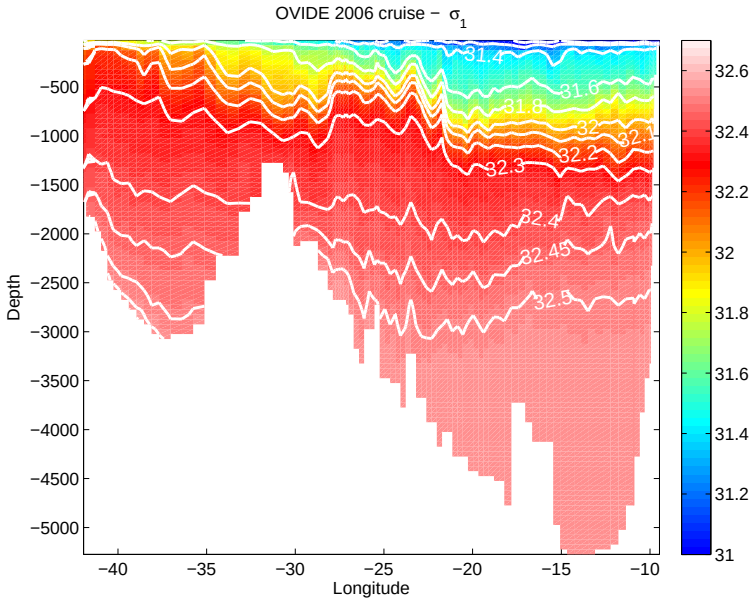

Figure 48: Density anomaly referenced at 1000 m in OVIDE 2006 section

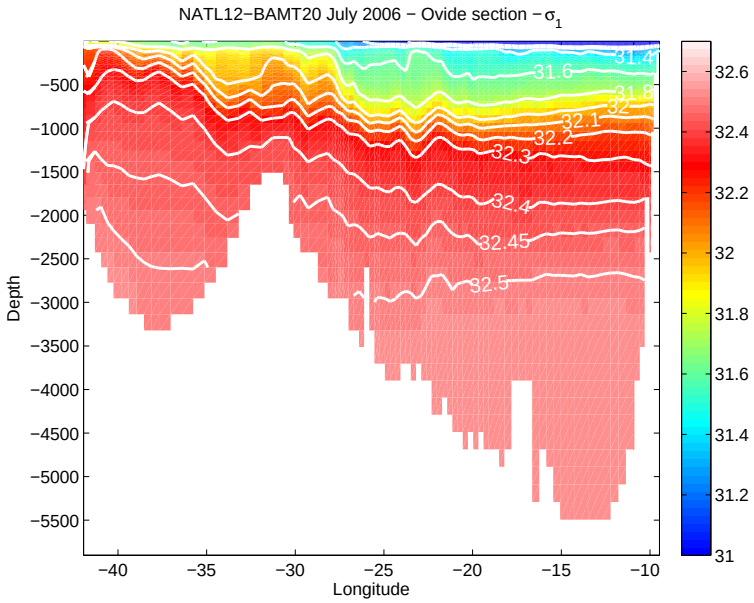

Figure 49: Density anomaly referenced at 1000 m in NATL12-BAMT20 along OVIDE 2006

10.4 Calcul du transport

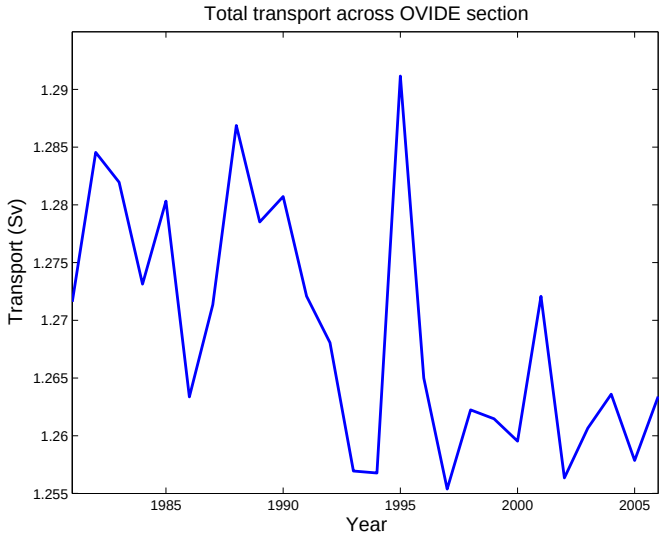

Figure 50: Transport in NATL12-BAMT20 along OVIDE 2006

References

[de Boyer Montegut et al.(2004)] de Boyer Montegut, C., et al., 2004: Mixed layer depth over the global ocean: An examination of profile data and a profile-based climatology. *J. Geophys. Res.*, **109**.

Ambar, I. and M. Howe, 1979: Observations of the Mediterranean outflow - I mixing in the Mediterranean outflow. *Deep Sea Research* 26A, 535-554.

Arhan M., A.M. Treguier, B. Bourles, S. Michel, 2006: Diagnosing the annual cycle of the Equatorial Undercurrent in the Atlantic Ocean from a general circulation model. *J. Phys. Oceanogr*, 36, 1502-1522.

Baringer, M.O., 1993: Mixing and dynamics of the Mediterranean outflow. PhD. thesis, MIT/WHOI, WHOI-93-52, 244pp.

Barnier, B., G. Madec, T. Penduff, J.M. Molines, A.M. Treguier, J. Le Sommer, A. Beckmann, A. Biastoch, C. Böning, J. Dengg, C. Derval, E. Durand, S. Gulev, E. Remy, C. Talandier, S. Theetten, M. Maltrud, J. McClean, B. De Cuevas 2006: Impact of partial steps and momentum advection schemes in a global ocean circulation model at eddy permitting resolution. *Ocean Dynamics*, p543-567, DOI: 10.1007/s10236-006-0082-1.

Brodeau, L., B. Barnier, A.M. Treguier, T. Penduff, S. Gulev, 2008: An ERA40-based atmospheric forcing for global ocean circulation models. *submitted to Ocean Modelling.*

Carton, X., L. Cherubin, J. Paillet, Y. Morel, A. Serpette and B. Le Cann, 2002 : Meddy coupling with a deep cyclone in the Gulf of Cadiz. *J. Mar. Syst*, **32**, p.13-42

Gourcuff, C., 2008 : Etude de la variabilité de la circulation du gyre subpolaire de l'Atlantique Nord à l'aide des données Ovide et des mesures satellitaires. Thèse de Doctorat de l'Université de Bretagne Occidentale.

Johnson G.C., T. B. Sanford, M. O'Neil Baringer, 1994: Stress on the Mediterranean outflow plume: part I. Velocity and water property measurements. *J. Phys. Oceanogr.*, 24, 2072-2083.

Ochoa, J. and N.A. Bray, 1991: Water mass exchange in the Gulf of Cadiz. Deep Sea Res., 38(Suppl 1), S465-S503. Treguier, A.M. 2008: DRAKKAR NATL12 model configuration for a 27-year simulation of the North Atlantic ocean. LPO report LPO-2008-05, 15pp.

Lherminier, P., H. Mercier, C. Gourcuff, M. Alvarez, S. Bacon, C. Kermabon, 2007 : Transports across the 2002 Greenland-Portugal Ovide section and comparison with 1997. *J. Geophys. Res. Oceans*, Vol. 112, DOI: 10.1029/2006JC003716.

Rhein M, and Hinrichsen H. H., 1993: Modification of Mediterranean water in the Gulf of Cadiz, studied with hydrographic, nutrient and chlorofluoromethane data. *Deep Sea Res.*, 40, pp 267-291.

Treguier, A.M., S. Theetten, E Chassignet, T. Penduff, R Smith, L Talley, C. Boning, J.O. Beismann, 2005 : The North Atlantic subpolar gyre in four high resolution models. *J. Phys. Oceanogr.*, 35, 757-774.